

¹⁰G. A. P. Engelbertink and J. W. Olness, *Bull. Am. Phys. Soc.* **15**, 566 (1970); and to be published.

¹⁴G. Chilosi, G. D. O'Kelley, and E. Eichler, *Nucl. Phys.* **A136**, 649 (1969).

¹²See, e.g., R. C. Greenwood, R. G. Helmer, and R. J. Gehrke, *Nucl. Instr. Methods* **77**, 141 (1970).

¹³D. E. Alburger and G. A. P. Engelbertink, to be published.

¹⁴Also note that if the Ca^{47} ground state has $J^\pi = \frac{7}{2}^-$ as is expected, then the reported branch (Ref. 1) of $\approx 1\%$ ($\log ft \approx 8.4$) for the decay of K^{47} to this state must certainly be in error, since a $\frac{1}{2}^+ \rightarrow \frac{7}{2}^- \beta^-$ transition is third forbidden and so must have a $\log ft$ at least several orders of magnitude larger than 8.4 (see Ref. 2).

¹⁵T. A. Hughes and M. Soga, *Nucl. Phys.* **A116**, 33 (1968).

¹⁶T. T. S. Kuo and G. E. Brown, *Nucl. Phys.* **A114**, 241 (1968).

¹⁷C. M. Lederer, J. M. Hollander, and I. Perlman, *Table of Isotopes* (John Wiley & Sons, Inc., New York, 1967), 6th ed.

¹⁸See, e.g., S. Hinds and R. Middleton, *Nucl. Phys.* **A92**, 422 (1967); P. D. Barnes, C. K. Bockelman, O. Hansen, and A. Sperduto, *Phys. Rev.* **140**, B42 (1965); J. L. Yntema and G. R. Satchler, *Ibid.* **161**, 1137 (1967); H. O. Funsten, N. R. Roberson, and E. Rost, *Ibid.* **134**, B117 (1964).

¹⁹The half-life of the Ti^{50} 3198-keV level has recently been measured using electronic timing of $\beta^- \gamma$ coincidences (S. Cochavi, D. B. Fossan, S. H. Henson, D. E. Alburger, and E. K. Warburton, to be published). The result of 630 ± 30 psec is consistent with $E2$ radiation and excludes the possibility of higher multipole orders.

²⁰Y. L. Yntema, *Phys. Rev.* **186**, 1144 (1969).

²¹See, G. Sartoris and L. Zamick, *Phys. Rev.* **167**, 1035 (1968).

Neutron Emission from the Zn^{64} Compound Nucleus Formed in Two Ways: $p + Cu^{63}$ and $\alpha + Ni^{60}\dagger$

Stuart T. Ahrens, William G. Simon, and Hudson B. Eldridge

Department of Physics, The University of Wyoming, Laramie, Wyoming 82070

(Received 16 March 1970)

The Zn^{64} compound nucleus was formed at an excitation energy of 33.3 MeV using two different target-projectile systems: 26.0-MeV protons on Cu^{63} and 31.3-MeV α particles on Ni^{60} . Neutrons were detected with nuclear emulsions using the internal-radiator method. Exposures were made simultaneously at the following angles: 18, 33, 90, 147, and 162°. The c.m. energy spectra (2–15 MeV) of the two systems are very nearly the same. For both systems symmetry about 90° in the c.m. angular distributions is seen up to about 6 MeV followed by a forward peaking at higher energies. The symmetric (compound-nuclear) parts of the angular distributions differ significantly in anisotropy. For the $p + Cu^{63}$ system the distribution is essentially isotropic while for the $\alpha + Ni^{60}$ system we have an average anisotropy of about 1.4. We also observe for the $\alpha + Ni^{60}$ system a slight but significant increase in anisotropy with energy of the emitted neutron (1.290 ± 0.047 at 2 MeV to 1.649 ± 0.119 at 6 MeV). The changes in average anisotropy, as we change target-projectile systems, are basically consistent with multiple-emission calculations using a rigid-sphere moment of inertia ($r_0 = 1.22$ F). The change in anisotropy with emission energy is not seen in the calculations. It is estimated that, for the $p + Cu^{63}$ and $\alpha + Ni^{60}$ systems, direct-reaction neutrons constitute 5 and 3% of the total observed neutron spectra.

I. INTRODUCTION

In order to isolate and study the role of angular momentum in the statistical decay of a compound nucleus, one often turns to a "Ghoshal-type experiment." Since Ghoshal did his classic work, in which he investigated the decay of the Zn^{64} compound nucleus formed with α particles and protons,¹ many other systems have undergone similar analysis.² The typical output of such experiments is usually of the form of either excitation functions or particle spectra.

This work is focused on the Zn^{64} compound nu-

cleus. For this system the low-energy-reaction excitation functions have been well established for several projectile-target combinations,¹⁻⁹ but the exact role of angular momentum is still uncertain.² Presented here are the results of a study in which the energy spectra (2–15 MeV) and angular distributions (18, 33, 90, 147, 162°) of emitted neutrons were measured and calculated for the reaction systems $p + Cu^{63}$ and $\alpha + Ni^{60}$, both of which lead to the Zn^{64} compound nucleus at an excitation energy of 33.3 MeV.

In Sec. II we cover the experimental procedures used and present the results. In Sec. III the mea-

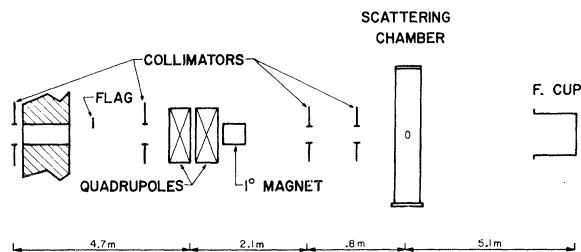


FIG. 1. Experimental arrangement.

sured neutron spectra for the two systems are compared with each other and then with multiple-emission calculations. Discussion is focused mainly on the anisotropy of the angular distributions: how it changes as one changes target-projectile systems and how it is dependent on emission energy.

II. EXPERIMENTAL PROCEDURES AND RESULTS

The irradiations were carried out at the University of Colorado 52-in. cyclotron. Nuclear emulsions (600- μ Ilford K5) were used to obtain the energy spectra and angular distributions of neutrons from 26.0-MeV protons on Cu^{63} and 31.3-MeV α particles on Ni^{60} . Target thicknesses were 2.76 and 1.08 mg/cm^2 , respectively.

In order to minimize background, the exposures were made in the "barn area," a very large open room with low-mass walls and a low-mass steel mat floor. The experimental arrangement (Fig. 1) is designed so that all unavoidable background sources such as collimators and the Faraday cup are as far as possible from the emulsions, while the emulsions are as close as is reasonably possible to the target. Background was estimated by comparing exposures made without a target to those made with a target. Depending on the particular run and angle this estimate varied from 1 to 4%. Corrections for background have been applied to the data.

The scattering chamber is shown in Fig. 2. In designing the chamber every effort was made to reduce the mass present in the regions around the target and around the emulsions. This "open geometry" reduces to a minimum the effects of secondary scattering of neutrons. The chamber was constructed from a stainless-steel tube 5 in. in diameter with 0.026-in. walls and 3 ft in length. The chamber was made long so that the relatively massive flanges are removed from the target-emulsion area. The beam entered the chamber through a $\frac{3}{4}$ -in.-diam, 0.15-in.-wall stainless-steel tube welded to the chamber. The exit tube was

made cone-shaped in order to reduce the amount of beam striking it due to multiple scattering in the target.

Multiple scattering also caused some of the beam to be scattered wide of the Faraday cup, necessitating corrections to the beam current. These corrections were checked in three ways. First, multiple-scattering calculations based on Molière's theory were used. Second, a brass foil was activated at the Faraday-cup position, and the distribution of activity on it was determined. This compared well with the calculations. Third, the ratio of target-in to target-out Faraday-cup readings was measured several times during each run, with the beam as steady as possible. Despite these precautions the absolute normalization was not always reproduced and we later compare only relative cross sections to theory.

Emulsions were placed horizontally on a $\frac{3}{84}$ -in.-thick aluminum ring outside the scattering chamber at a minimum distance of 2.8 in. from the target (Fig. 2). The plane of the emulsions is below that of the target and thus the neutrons enter the surface of the emulsion at an angle of about 15° . This allowed any part of the emulsions to be scanned without the need to correct for attenuation of neutrons by the emulsion. Three emulsions were used on each side of the beam and all were simultaneously exposed. The emulsions were wrapped first with a 0.001-in. layer of Teflon.

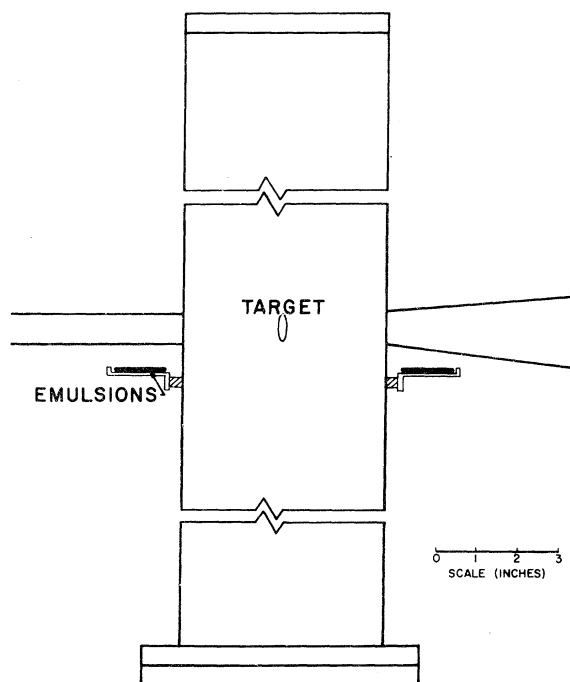


FIG. 2. Scattering chamber.

This provided a chemically inert and hydrogen-free cover. This was followed by a double layer of 0.0005-in. aluminum foil which formed a light-tight cover.

In order to eliminate charged particles coming from the target that would otherwise intercept the emulsion, a 0.200-in. aluminum collar was placed around the scattering chamber such that it would cast a shadow on the emulsions. In the worst case, 12% of the neutrons interact in passing through this absorber. The effect of these interactions is not simply to attenuate the neutron flux, since "in-scattering" occurs with comparable magnitude. Corrections for these effects were not made. Owing to symmetry about the vertical axis of the chamber it is expected that the spectra will be affected in the same way at all angles. Therefore, we believe that the angular distributions are only slightly changed by this source of error.

The energy E_p of protons elastically scattered by neutrons in the emulsion is given by $E_p = E_n \times \cos^2\theta$, where E_n is the neutron energy and θ is the angle between the directions of the neutron and proton. Thus, a measurement of the proton range and the angle of the track with respect to the direc-

tion of the incident neutron enables one to determine the energy of the neutron.

The scanning was done with a digitized microscope, which records the x, y, z coordinates of points in the emulsion on IBM cards. Coordinates were recorded at the beginning and end of each track and at intermediate points as necessary to define the path of the proton adequately. The range and scattering angle of each proton recoil could then be determined directly from these measure-

TABLE I. Experimental cross sections for neutron production by 26.0-MeV protons on Cu⁶³ and 31.3-MeV α particles on Ni⁶⁰. Errors given are statistical.

θ_{lab} (deg)	$p + Cu^{63}$		$\alpha + Ni^{60}$	
	E_n (MeV)	$\frac{d^2\sigma}{d\Omega dE}$ (mb/MeV sr)	E_n (MeV)	$\frac{d^2\sigma}{d\Omega dE}$ (mb/MeV sr)
18	1.46	17.98 ± 0.56	1.49	35.29 ± 1.23
	2.44	15.04 ± 0.59	2.48	26.34 ± 1.25
	3.45	10.61 ± 0.55	3.44	21.02 ± 1.23
	4.79	5.43 ± 0.32	4.85	12.34 ± 0.76
	6.85	2.81 ± 0.26	6.78	5.06 ± 0.56
	8.75	1.17 ± 0.19	8.98	4.27 ± 0.58
	10.81	1.10 ± 0.20	11.13	1.44 ± 0.37
	13.88	0.81 ± 0.14	13.65	1.02 ± 0.25
33	1.47	17.08 ± 0.38	1.48	30.65 ± 0.96
	2.46	13.72 ± 0.40	2.43	24.33 ± 0.99
	3.46	9.92 ± 0.38	3.46	16.90 ± 0.92
	4.83	5.56 ± 0.22	4.81	9.06 ± 0.54
	6.91	2.31 ± 0.16	6.76	4.25 ± 0.42
	8.91	1.22 ± 0.14	8.93	2.52 ± 0.37
	10.85	0.80 ± 0.13	10.69	1.06 ± 0.26
	13.94	0.57 ± 0.09	13.56	0.48 ± 0.15
90	1.45	15.47 ± 0.32	1.46	21.53 ± 0.66
	2.46	11.68 ± 0.32	2.44	17.46 ± 0.69
	3.45	7.65 ± 0.29	3.41	10.67 ± 0.60
	4.77	3.89 ± 0.16	4.76	5.04 ± 0.34
	6.80	1.54 ± 0.12	6.74	1.88 ± 0.24
	8.88	0.88 ± 0.11	8.85	0.87 ± 0.18
	10.84	0.36 ± 0.07	10.69	0.32 ± 0.12
	13.50	0.25 ± 0.05	13.74	0.18 ± 0.07
147	1.46	13.72 ± 0.39	1.45	22.88 ± 0.68
	2.44	10.44 ± 0.40	2.45	16.57 ± 0.67
	3.44	6.24 ± 0.34	3.45	8.89 ± 0.54
	4.80	3.58 ± 0.20	4.74	4.51 ± 0.32
	6.83	0.93 ± 0.12	6.76	1.50 ± 0.21
	9.00	0.27 ± 0.08	8.61	0.51 ± 0.14
	10.45	0.16 ± 0.07	10.87	0.18 ± 0.09
	13.91	0.13 ± 0.05	13.25	0.09 ± 0.05
162	1.44	13.98 ± 0.48	1.44	23.16 ± 0.76
	2.45	10.10 ± 0.47	2.45	17.20 ± 0.76
	3.45	7.41 ± 0.45	3.44	10.09 ± 0.65
	4.79	3.94 ± 0.27	4.82	5.36 ± 0.38
	6.97	0.88 ± 0.14	6.79	1.76 ± 0.25
	8.81	0.75 ± 0.15	8.95	0.27 ± 0.11
	10.96	0.44 ± 0.13	11.39	0.22 ± 0.11
	14.22	0.08 ± 0.04	12.51	0.07 ± 0.05

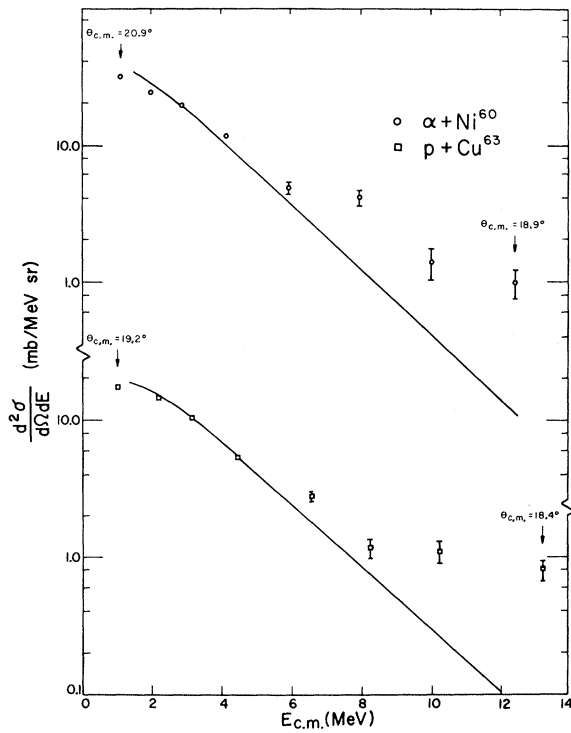


FIG. 3. Center-of-mass neutron energy spectrum, $\theta_{lab} = 18^\circ$. Center-of-mass angles are shown for the most extreme energies represented. Errors shown are statistical. Curves are from multiple-emission calculations normalized to experiment at (3 MeV, 90°).

ments. In the neutron energy range considered in this study, the energy resolution of the scanning system is estimated to be about 0.5 MeV. Further details on the scanning are discussed elsewhere.¹⁰

For both reactions, neutron spectra were measured at $\theta_{lab} = 18, 33, 90, 147,$ and 162° . The results are shown in Table I. Each of these data points was then transformed to the center-of-mass (c.m.) system (Figs. 3-7). Keeping track of the c.m. angles calculated in the transformation, these results were interpolated at integer energies from 2 to 13 MeV to give the angular distributions. These are seen in part in Figs. 8 and 9.

III. DISCUSSION

For both systems symmetry about 90° in the c.m. angular distributions (Figs. 8 and 9) is seen up to about 6 MeV, followed by a forward peaking at higher energies. The symmetric (compound-nuclear) parts of these distributions differ significantly in anisotropy. For the $p + Cu^{63}$ system we have essentially an isotropic distribution, while for the $\alpha + Ni^{60}$ system we have an average anisotropy of about 1.4. The angular distributions for the $\alpha + Ni^{60}$ system have been least-squares-fitted to the form $a + b \cos^2\theta$ and the anisotropies based on these fits are given in Table II. It is noted that a slight but significant increase in anisotropy with

energy of the emitted neutrons is observed.

Each c.m. energy spectrum (Figs. 3-7) contains measurements at slightly different c.m. angles. No appreciable error is introduced if we consider these measurements to correspond to the average angle represented in the system. The low-energy (compound-nuclear) parts of the energy spectra for the $\alpha + Ni^{60}$ system have one interesting feature which follows from the anisotropy calculations. Namely, since the observed anisotropies for this system are energy dependent, it follows that these parts of the energy spectra are angle dependent, being steepest at 90° .

Using the evaporation program of Reames,¹¹ we have calculated neutron energy and angular distributions for both systems. This program is based on the semiclassical formalism developed by Ericson and Strutinski¹² and Ericson.¹³ It was written originally to follow, in an "average-value" way, the multiple-emission process in compound nuclei formed by energetic heavy ions. It is important to keep in mind that this program has several general weaknesses. First, as has been argued by Thomas,¹⁴ the average-value procedure used to follow the multiple emission loses track of much that may be important in terms of angular momentum effects. Second, this program ignores all γ -ray

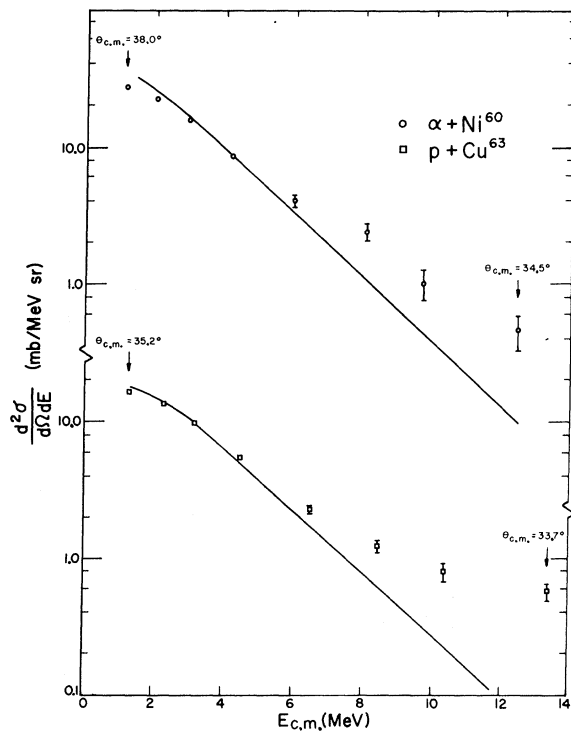


FIG. 4. Center-of-mass neutron energy spectrum, $\theta_{lab} = 33^\circ$. (See Fig. 3.)

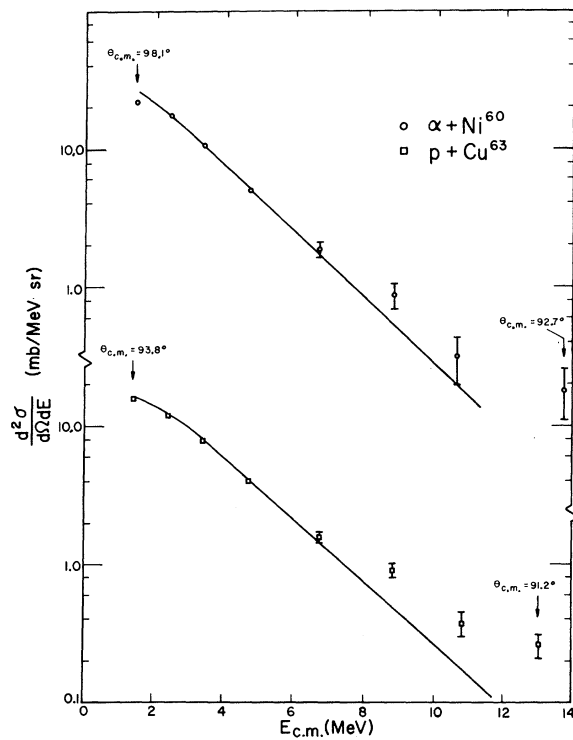


FIG. 5. Center-of-mass neutron energy spectrum, $\theta_{lab} = 90^\circ$. (See Fig. 3.)

competition. The importance of γ -ray competition on neutron emission, for example, has been shown in the study of the Po^{210} compound system.¹⁵ Next, this program calculates transmission coefficients using the inverted harmonic-oscillator formula of Hill and Wheeler.¹⁶ We believe that for charged particles near the Coulomb barrier the transmission coefficients are rather inaccurate. Nevertheless, some features of the neutron spectra are little affected by these weaknesses. An examination of each of these three approximations indicates, for instance, that a more accurate calculational procedure which uses the Ericson formalism would give about the same angular distributions for neutrons. Finally, we point out that the Ericson formalism is a classical one, and other more detailed, quantal formalisms have been developed.¹⁴

We have employed, except in the moment-of-inertia calculations, the same parameters that Reames used in calculating emission spectra from heavy-ion bombardment.¹¹ We have taken the moment of inertia to be that of a rigid sphere, $\mathcal{I} = \mathcal{I}_{rigid} = 0.4 m_0 r_0^2 A^{5/3}$, where m_0 is the nucleon mass, r_0 is the radius parameter, and A is the mass number. The calculated anisotropies are most affected by a change in r_0 . We adjusted r_0 such that for the $\alpha + Ni^{60}$ system the calculated anisotropy agreed with the measured value at 3

TABLE II. Energy dependence of anisotropy for neutrons from $\alpha + Ni^{60}$.

Neutron energy	Experimental anisotropy (Ref. a)	Theoretical anisotropy (Ref. b)
0.5		1.39
1.5		1.39
2.0	1.290 ± 0.047	1.41
3.0	1.419 ± 0.087	1.42
4.0	1.462 ± 0.154	1.43
5.0	1.619 ± 0.152	1.41
6.0	1.649 ± 0.179	1.42

^a Determined by a least-squares fit of the form $a + b \cos^2 \theta$.

^b Determined from calculations using a rigid-sphere moment of inertia with $r_0 = 1.22$. See text.

MeV. This yielded a value of $r_0 = 1.22$ F. Most recent investigators have assumed r_0 to be between 1.20 and 1.25 F. The energy and angular spectra calculated with $r_0 = 1.22$ F are shown with the experimental results in Figs. 3–9. For both systems theory is normalized to experiment at the coordinates (3 MeV, 90°). The calculated energy spectra correspond to the average angle represented in the measured spectrum. The calculated spectra show noticeably different behavior at low

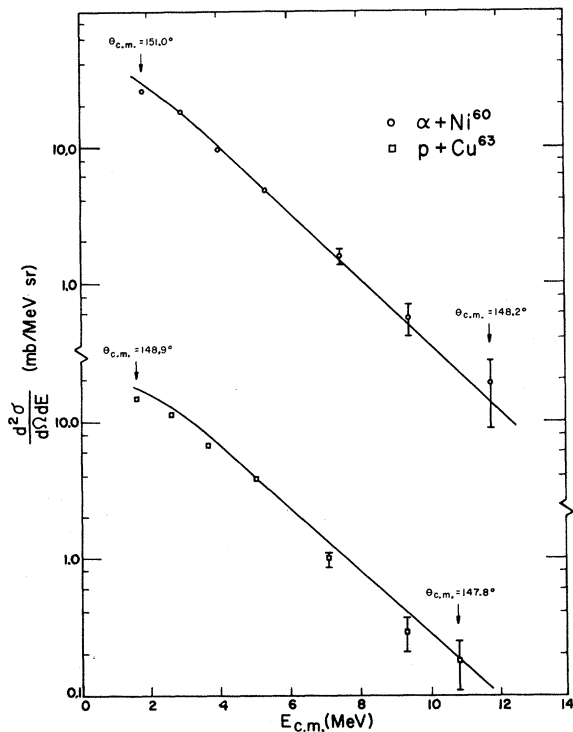


FIG. 6. Center-of-mass neutron energy spectrum, $\theta_{lab} = 147^\circ$. (See Fig. 3.)

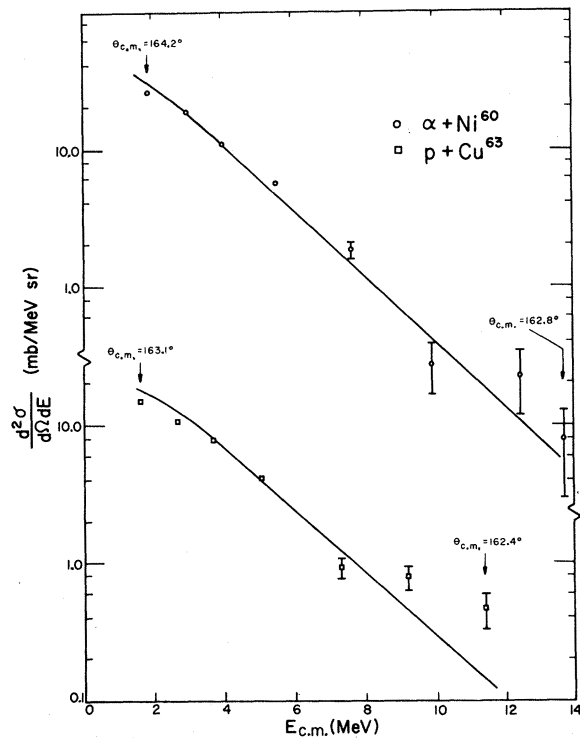


FIG. 7. Center-of-mass neutron energy spectrum, $\theta_{lab} = 162^\circ$. (See Fig. 3.)

energies, the α -particle-induced spectra showing more low-energy neutrons. By comparing the calculated and measured energy spectra above 6 MeV, it is estimated that for the $p + \text{Cu}^{63}$ and $\alpha + \text{Ni}^{60}$ systems direct-reaction neutrons constitute 5 and 3% of the total observed neutron spectra. The calculated angular distributions show approximately the same change in anisotropy (as we change target-projectile systems) as the interpolated experimental values.

Thus, these multiple-emission calculations based on a rigid-sphere moment of inertia ($r_0 = 1.22 \text{ F}$) are basically consistent with our measured neutron spectra. This is in contrast to the conclusions of Smith² who has measured the (x, n) , $(x, 2n)$, and (x, pn) excitation functions for the $p + \text{Cu}^{63}$ and $\alpha + \text{Ni}^{60}$ systems. In that work a displacement of the excitation functions for the $p + \text{Cu}^{63}$ system relative to the excitation functions for the $\alpha + \text{Ni}^{60}$ system was noted and ascribed to angular momentum effects. Using the position of the Zn^{64} photoexcitation curves of Sagane⁹ as reference points, and the calculated spin-average angular

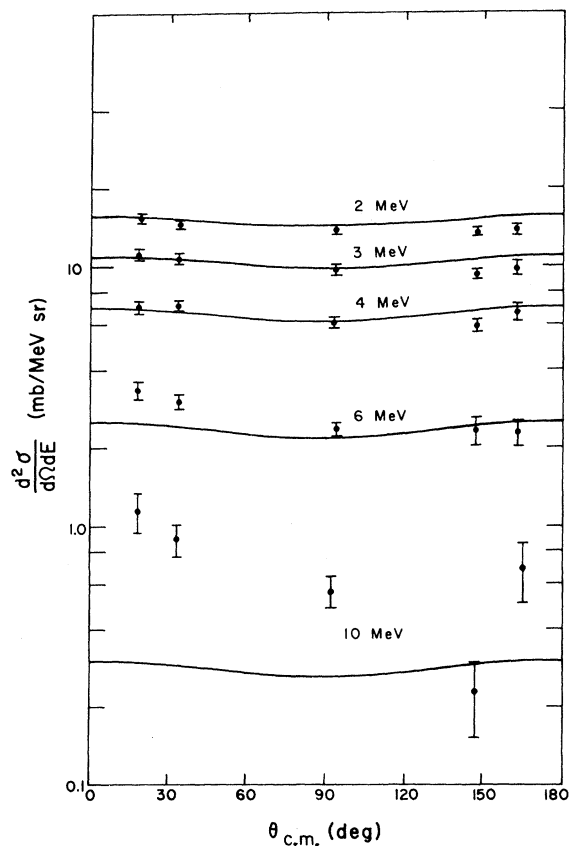


FIG. 8. Center-of-mass neutron angular distributions for $p + \text{Cu}^{63}$. Errors shown are statistical. Curves are multiple-emission calculations normalized to experiment at (3 MeV, 90°).

momenta of the compound systems, Smith calculated the moments of inertia for the two systems. He concluded from this study that for the $\alpha + \text{Ni}^{60}$ system $\mathcal{I} = \mathcal{I}_{\text{rigid}}(r_0 = 1.25 \text{ F})$ while for the $p + \text{Cu}^{63}$ system $\mathcal{I} = 0.3\mathcal{I}_{\text{rigid}}(r_0 = 1.25 \text{ F})$. When the multiple emission calculations for the $p + \text{Cu}^{63}$ system were repeated with $\mathcal{I} = 0.3\mathcal{I}_{\text{rigid}}(r_0 = 1.22 \text{ F})$ and $\mathcal{I} = 0.3\mathcal{I}_{\text{rigid}}(r_0 = 1.50 \text{ F})$, the average anisotropy was found to be 1.7 and 1.4, respectively. These values are clearly in disagreement with the essentially isotropic distributions which we found for this target-projectile system. As stated earlier, we do not believe that this result would be altered significantly if a more detailed analysis using the Ericson formalism were used.

For both systems the calculated anisotropies show very little change with energy of the emitted neutron. As seen in Table II, this result is not supported by our measured values for the $\alpha + \text{Ni}^{60}$ system. Other measurements¹⁷⁻²² give mixed results for this dependence: some showing an increase in anisotropy with emission energy, while others show a decrease.

Thomas¹⁴ has pointed out that there are two opposing effects which give an energy dependence to

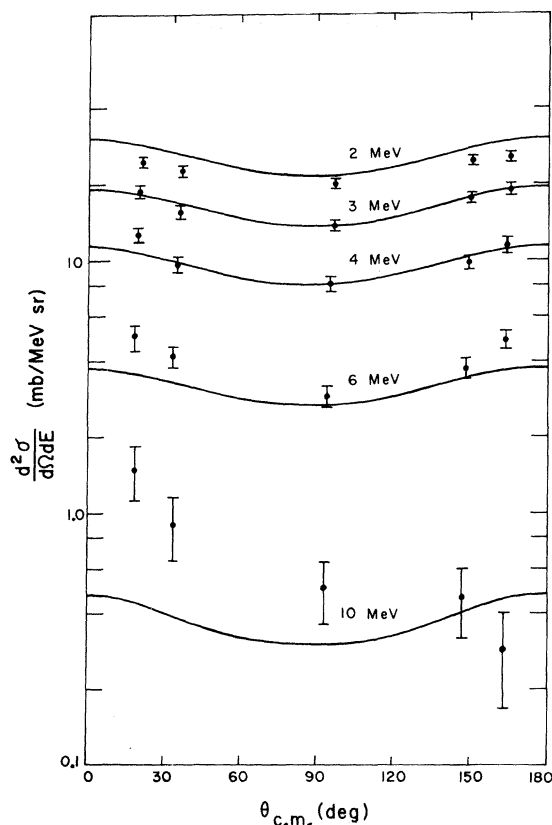


FIG. 9. Center-of-mass neutron angular distributions for $\alpha + \text{Ni}^{60}$. (See Fig. 8.)

the anisotropy. First, the coupling between the angular momentum J of the compound system and the orbital angular momentum l of the emitted particle increases with increasing l . Thus, for a given stage of evaporation, the anisotropy of the emitted particle increases with particle energy. Second, as the evaporation chain proceeds, there becomes a scarcity of high-angular-momentum states in the residual nucleus. As a consequence there is a larger coupling between l and J and larger anisotropies result for particles emitted in the latter stages of evaporation. Thus if the first effect dominates, the anisotropy should increase with emitted-particle energy, while if the latter effect dominates we should find the opposite dependence.

Upon looking at the intermediate results from Reames's calculations for the $\alpha + \text{Ni}^{60}$ system, we see that both of these effects are large, but that a cancellation results in essentially no change in

anisotropy with energy. For another system, Ni-(C¹², xn) with 120-MeV C¹² ions, Reames's program shows a decrease in anisotropy with energy up to 6 MeV and an increase above this value. Thus both effects are in evidence in the same spectrum. We conclude that it appears possible for anisotropies to increase with energy, decrease with energy or do both, showing a minimum value at some energy.

ACKNOWLEDGMENTS

We are grateful to the staff members of the University of Colorado Nuclear Physics Laboratory, especially D. A. Lind, for making the emulsion exposures possible. We also would like to thank J. Thomas who helped with the construction of the beam-transport system, F. L. Simon and J. Schock did much of the computer programming, and J. Burnett and K. Acott did most of the emulsion scanning.

†Work supported by the U. S. Atomic Energy Commission.

¹S. N. Ghoshal, Phys. Rev. **80**, 939 (1950).

²C. F. Smith, Jr., University of California Lawrence Radiation Laboratory Report No. UCRL-11862, 1965 (unpublished). A survey of 11 such systems is found in Table VIII of this reference.

³F. K. McGowan, P. H. Stelson, and W. G. Smith, Bull. Am. Phys. Soc. **5**, 266 (1960).

⁴J. W. Meadows, Phys. Rev. **91**, 885 (1953).

⁵H. A. Howe, Phys. Rev. **109**, 2083 (1960).

⁶J. P. Blaser, F. Boehm, P. Marmier, and D. C. Peaslee, Helv. Phys. Acta **24**, 3 (1951).

⁷B. L. Cohen and E. Newman, Phys. Rev. **99**, 718 (1955).

⁸S. Tanaka, J. Phys. Soc. Japan **15**, 2159 (1960).

⁹R. Sagane, Phys. Rev. **85**, 926 (1952).

¹⁰W. G. Simon and S. T. Ahrens, Phys. Rev., to be published.

¹¹D. V. Reames, Phys. Rev. **137**, B332 (1965).

¹²T. Ericson and V. Strutinski, Nucl. Phys. **8**, 284 (1958); **9**, 689 (1959).

¹³T. Ericson, Advan. Phys. **9**, 424 (1960).

¹⁴T. D. Thomas, Ann. Rev. Nucl. Sci. **18**, 343 (1968).

¹⁵J. R. Grover and R. J. Nagle, Phys. Rev. **134**, B1248 (1964).

¹⁶D. L. Hill and J. A. Wheeler, Phys. Rev. **89**, 1102 (1953).

¹⁷C. E. Hunting, Phys. Rev. **123**, 606 (1961).

¹⁸N. O. Lassen and V. A. Sidorov, Nucl. Phys. **19**, 579 (1965).

¹⁹D. M. Drake, Ph.D. thesis, University of Washington, 1962 (unpublished).

²⁰R. W. West, Ph.D. thesis, University of Washington, 1962 (unpublished).

²¹J. Benveniste, G. Merkel, and A. Mitchell, Phys. Rev. **174**, 1357 (1968).

²²M. J. Fluss, J. M. Miller, J. M. D'Auria, N. Dudgey, B. M. Foreman, Jr., L. Kowalski, and R. C. Reedy, Phys. Rev. **187**, 1449 (1969).